JOURNAL OF GEOPHYSICAL RESEARCH, VOL. 104, NO. D6, PAGES 6549–6562, MARCH 27, 1999

Application of the NCAR Regional Climate Model to eastern Africa 2. Simulation of interannual variability of short rains

Liqiang Sun,[1] Fredrick H. M. Semazzi,[2] Filippo Giorgi,[3] and Laban Ogallo[4]

Abstract. We have applied the NCAR RegCM2 to the simulation of the interannual variability of precipitation over eastern Africa for the short-rains season by performing a set of experiments for the years 1982 to 1993. The model reproduced the observed interannual variability of precipitation in most of the years. The results show that remote factors play a dominant role in determining the precipitation anomalies. Interannual variability of precipitation over Tanzania is closely related to El Niño events in their mature phase and sea surface temperature (SST) anomalies over the Indian and Atlantic Oceans. The southward shift of the Arabian High results in a southward shift of the zonal component of the Intertropical Convergence Zone (ITCZ), which is responsible for early onset of the rainy season (e.g., 1982 and 1986). The enhanced St. Helena High and weaker Mascarene High lead to the eastward shift of the meridional branch of the ITCZ for the wet years. Model simulations confirmed a strong positive correlation between precipitation anomalies over Lake Victoria and the warm El Niño-Southern Oscillation events, by which enhanced moist westerly flow from the Atlantic Ocean and the mainly easterly flow from the Indian Ocean converge over Lake Victoria during wet years. The interannual variability of precipitation over Lake Victoria and the western Kenya Highlands (WKH) are strongly coupled. Positive precipitation anomalies over the WKH region are usually associated with weaker Arabian High and Mascarene High, which weaken the large-scale divergence over the WKH region and favor the development of convection. The interannual variability of precipitation over eastern Kenya Highlands (EKH) is not directly related to the El Niño events, but the association with a warm SST anomaly pattern over the western Indian Ocean is evident during wet years. An El Niño signal is, however, evident for wet years over the Turkana Channel, warm SST anomalies over the northern Indian Ocean contribute enhanced water vapor transport over the region.

1. Introduction

In a companion paper by *Sun et al.* [this issue] the NCAR Regional Climate Model (RegCM2) was successfully customized for the region of eastern Africa, and its performance in simulating the intraseasonal climate variability during the short rains of 1988 was examined. Here we explore the ability of the RegCM2 to reproduce the interannual climate variability over eastern Africa and investigate the mechanisms responsible for the interannual variability. The model domain (Figure 1b) is characterized by two distinct climate regimes based on observed precipitation data [*Nicholson et al.*, 1988]. East Africa (i.e., the eastern portions of the domain) exhibits high interannual variability of precipitation. The standard departure of annual precipitation is generally more than 30% of its annual precipitation. Conversely, the Congo Basin and Angola plateau (i.e., the western portions of the domain) show relatively low interannual variability of precipitation, with a standard departure of annual precipitation of less than 15% of the mean [*Nicholson et al.*, 1988]. We mainly focus on the region of East Africa in this paper.

Many studies have been carried out in an attempt to identify the causes of the interannual rainfall variability over East Africa. Several investigations have focused on the importance of westerly flow over the region [*Johnson and Morth*, 1960; *Nakamura*, 1969; *Davis et al.*, 1985]. Enhanced westerly flow with incursion of humid Congo air played a role in the 1961/1962 floods [*Anyamba*, 1984] and in the wet conditions of 1977/1978 [*Minja*, 1985]. However, there are examples of such westerlies being associated with anomalously dry conditions, especially over eastern Kenya [*Nakamura*, 1969; *Kiangi and Temu*, 1984]. Several studies have focused on the influence of the convergence zones which affect the region, namely the Intertropical Convergence Zone (ITCZ) and the Congo air boundary. These may be intensified in response to changes in the subtropical highs, the westerly flow, or other regional dynamical factors [*Anyamba and Ogallo*, 1985].

A number of recent studies have demonstrated some interesting interactions between atmospheric and oceanic phenomena. Abnormally high sea surface temperatures (SSTs) over the equatorial Atlantic Ocean and central Indian Ocean were clearly linked to the heavy floods in October and November 1961. The SSTs over the above region remained high throughout the wet period from 1961 to 1963 [*Flohn*, 1987; *Nicholson*, 1989]. Teleconnections between rainfall and the SSTs over the

[1]Scripps Institution of Oceanography, University of California, San Diego, La Jolla.
[2]Department of Marine, Earth and Atmospheric Sciences, and Department of Mathematics, North Carolina State University, Raleigh.
[3]National Center for Atmospheric Research, Boulder, Colorado.
[4]Department of Meteorology, Nairobi Univrsity, Nairobi, Kenya.

Paper number 1998JD200050.
0148-0227/99/1998JD200050$09.00

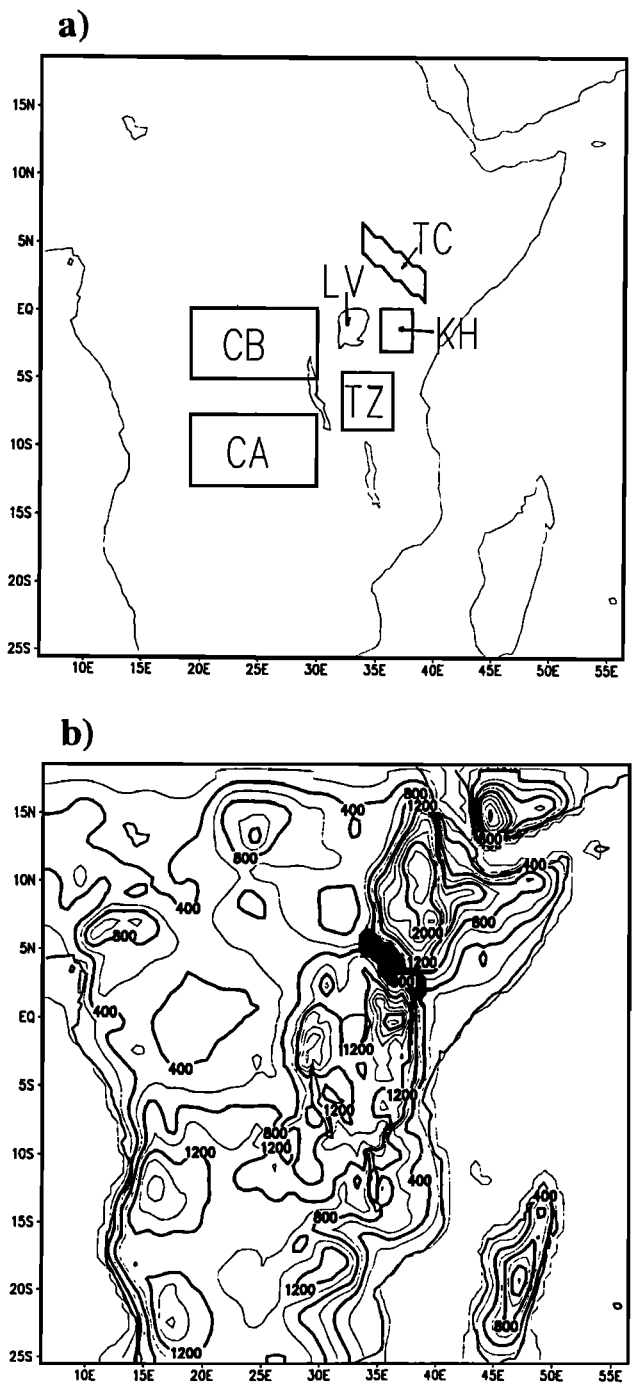

Figure 1. Six climatic subregions used for the evaluation of RegCM2 over eastern Africa: CB, Congo Basin; CA, southern Congo and Angola plateau; LV, Lake Victoria; TC, Turkana channel; KH, Kenya Highlands; and TZ, Tanzania; (b) model topography. Units are meters.

Pacific Ocean are also apparent [*Ogallo et al.*, 1988]. *Nicholson* [1996] identified a relationship between precipitation over East Africa and global SSTs based on observed data between 1946 and 1979. The October–December wet minus dry composite of SST indicated positive anomalies over most of the Indian Ocean, especially in the west, the equatorial region and mid-latitudes of the Pacific Ocean, negative anomalies over the subtropics of the Pacific Ocean, and a banded structure over most of the Atlantic Ocean.

Nicholson and Entekhabi [1987], *Ropelewski and Halpert* [1987], *Ogallo* [1988], and *Farmer* [1988] have all demonstrated a relationship between East African precipitation and the El Niño-Southern Oscillation (ENSO) phenomenon. A positive precipitation anomaly tends to occur during the short rains of warm ENSO events, while dry conditions prevail during the long rains of the following year and the short rains of the year prior to warm ENSO events [*Nicholson*, 1996].

It is interesting to note that the short rains contribute disproportionately to the interannual variability of precipitation. The correlation coefficient between annual totals and short rains exceeds 0.5 over most of East Africa [*Nicholson*, 1996]. The precipitation anomaly links to SSTs are stronger for the short rains than for the long rains, and the strongest effect of ENSO appears to be during the short rains [*Ogallo et al.*, 1988]. Also, the intermonth correlations of the rainfall during the short-rains season are high [*Ininda*, 1994]. The high correlations suggest high persistence in the factors that influence the temporal rainfall variations during the short-rains season. In this paper our investigation will thus focus on the short rains. The model domain and configuration is the same as those in the Experiment 9 of *Sun et al.* [this issue]. Figure 1b shows the model topography at 60 km grid point spacing. The simulation period is October, November, and December in each year from 1982 to 1993. For each year, the numerical experiment started from the initial conditions taken from September 1, European Center Medium-Range Weather Forecasts (ECMWF) reanalysis, and each model integration is 4 months, thus terminating at the end of December. The first month (i.e., September) is neglected to allow for model spin-up. The lateral boundary conditions for wind, temperature, water vapor, and surface pressure are interpolated from 6 hourly 14-pressure level ECMWF reanalysis. Time-dependent sea surface temperature is interpolated from a time series of observed monthly mean data on a grid of 2° × 2° resolution [*Shea et al.*, 1992]. Soil moisture is initialized as the same for every year simulation. A detailed description of the model is reported by *Sun et al.* [this issue], so it is not presented here. In section 2 we directly discuss the simulation results, while the main conclusions are summarized in section 3.

2. Simulation Results

The six regions defined by *Sun et al.* [this issue] are central Tanzania (TZ), Lake Victoria (LV), Kenya Highlands (KH), Turkana channel (TC), Congo Basin (CB), and southern Congo and Angola (CA) plateau (see Figure 1a). Composite analysis is adopted to investigate the possible causes of the precipitation variability over most of the regions. The primary criteria for the composite analysis is based on the "wet" and "dry" stratification of short rains for each region. We obtain the precipitation anomaly for an individual year by removing 12-year average precipitation. Four distinctly wet (dry) short-rains seasons are then extracted from the anomaly time series. The "wet" and "dry" seasonal composites are obtained by averaging the four seasons of each category. Wet minus dry composite analysis is adopted in our study, and it has the following advantages:

1. It increases the magnitude of the composite values in regions where the wet and dry periods have opposite signals, while in regions where the wet and dry periods have the same signals, the composite value is small.

2. Since the number of degrees of freedom is increased

Table 1. List of Years Used for Composite Analysis for Various Regions.

	1982	1983	1984	1985	1986	1987	1988	1989	1990	1991	1992	1993
TZ	W		D	D	W	D		W			W	D
LV	W			D	W		D	W		W	D	D
WKH	W	W		D	D		D	W			W	D
EKH	W	D		D	W	D	W		W			D
TC	W		D	D		D	W	D		W	W	

WKH is the Lake Victoria side of the Kenya Highlands, and EKH is the Indian Ocean side of the Kenya Highlands. W, wet; D, dry.

when the wet minus dry composite is used, more values are likely to be statistically significant as compared to either the wet or the dry composite alone, thus increasing the variable significance [*Ward*, 1992].

3. The wet minus dry composite can be used to identify regions where consistent variations occurred in at least a number of composite years.

The wet minus dry composite analysis, however, has several limitations. Such as the following:

1. If some of the years in the composite are taken from within a period of persistent precipitation anomaly, the composite may contain the influence of processes that operate on both interdecadal timescale and interannual timescale [*Ward*, 1992].

2. Because only four seasons are used in the composites, the results may be greatly influenced by just one season in which the ocean-atmosphere anomalies are very large. We will eliminate this kind of season in our composite analysis by choosing another year to take its place. If there is no more year to choose, we will reduce the composite to two members.

3. In different years the seasonal rainfall anomalies may result from different causes, which may have different signals in the ocean-atmosphere variables. Thus the composite analysis sometimes may fail to present the teleconnection structures [*Ward*, 1992]. We will analyze the anomaly at each individual season before applying for the composite analysis to avoid this kind of shortcoming.

Although the simulation period from October to December in each year represents the seasonal transition from southeast monsoons to northeast monsoons over East Africa, high temporal coherence in the monthly precipitation within the short-rains season were observed [*Ogallo*, 1989]. Thus the analysis will be based on the full seasonal average. The years used for composite analysis for the various regions are listed in Table 1. There are no two regions which share all the same years in the composite analysis. Therefore no one region among the five regions is homogeneous to the others. However, the composites for different regions do share many of the same years. This suggests that there are some common factors that affect the interannual variability of rainfall over different regions.

2.1. Tanzania

The central Tanzania region is a relatively large homogeneous region [*Nicholson et al.*, 1988], which includes 111 model grid points. Observations show that Tanzania is usually dry in October and wet in December. The onset of the rainy season occurs in November. The precipitation stations available for this study over central Tanzania are listed in Table 2. The 18-station 12-year mean observed precipitation for October–December is 293.8 mm. The 12-mean simulated precipitation is 275.1 mm. This mean was obtained by first interpolating the simulated precipitation to the station locations listed in Table 2 and then averaging the interpolated values. The model simulation is thus slightly drier than the observations.

Fig. 2 shows the observed precipitation anomalies from the 12-year observed mean and the simulated precipitation anomalies from the 12-year simulated mean. The correlation coefficient r between the simulated precipitation anomalies and the observed precipitation anomalies is 0.802. The critical correction coefficient r_c calculated on the basis of student's t-tests at 1% significant level is 0.708. This result indicates that the simulated and observed precipitation anomalies are significantly correlated at the 1% significance level during the 12 years. The observed wet conditions in 1982, 1986, 1989, and 1992 and dry conditions in 1984, 1985, 1987, 1988, 1991, and 1993 are reproduced in the model simulation. The severely dry conditions in 1987 are underestimated, and dry conditions in 1985 are exaggerated in the model simulation, although the model produces the correct sign of the precipitation anomalies. The model fails to simulate the moderately dry conditions in 1983 and 1990. Overall, the interannual variability of precipitation is generally captured by the model.

To validate the model performance, we analyze not only the total amount of precipitation but also the daily precipitation intensity distribution. The observed daily precipitation data were available only for five stations over Tanzania (i.e., Tabora, Dodoma, Morogoro, Iringa, and Mbeya). Figure 12 of the companion paper [*Sun et al.*, this issue] showed that the simulated daily precipitation in 1988 is generally consistent with observations. Because of the large gaps in the daily observations, we calculated the correlation coefficient between the simulated and the observed daily precipitation instead of

Table 2. Details of Precipitation Stations Over Central Tanzania

Station	Latitude, °S	Longitude, °E	Elevation, m
Nzega	4.13	33.11	1219
Mwanhala	4.24	33.09	1250
Ndala Mission	4.45	33.16	1372
Singda District Office	4.48	34.45	1498
Itaga Seminary	4.53	32.44	1219
Tabara	5.05	32.50	1182
Manyoni District Office	5.44	34.50	1248
Dodoma	6.10	35.46	1120
Mpwapwa Research Station	6.20	36.30	1037
Morogoro	6.50	37.39	526
Iringa	7.38	35.46	1428
Mkulwe Mission	8.32	32.18	1067
Chunya Agriculture	8.32	33.25	1493
Kilima Estate	8.35	35.20	1859
Kidope Mufindi	8.37	35.15	1981
Kwiro Mission	8.40	36.40	1006
Mahenege Hospital	8.41	36.43	1106
Mbeya	8.56	33.28	1758

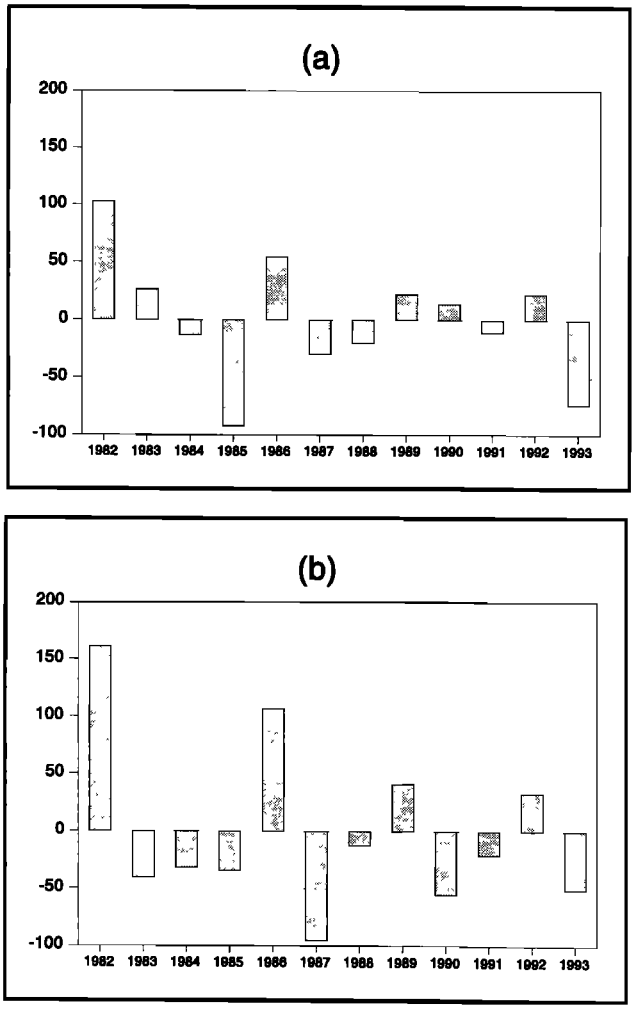

Figure 2. Precipitation anomalies from the 12-year mean over Tanzania for the October–December season: (a) model simulation, and (b) observations. Units are in millimeters.

giving the time series of the daily precipitation. The correlation in 1988 is also listed in Table 3. The numbers of days with observed precipitation data during short rains are listed in Table 3.

The correlation between the simulated and the observed daily precipitation (Table 2) shows that the simulated and observed daily precipitation are significantly correlated at the 1% significance level for all the years except 1990. This result indicates that the model captures the daily variations of precipitation in most of the years. We note that the model simulates the daily variation of precipitation well in 1983 although it fails to reproduce the total precipitation anomaly during the short rains in the same year. The model fails to reproduce not only the total precipitation anomaly but also the temporal variation of precipitation for 1990.

Four wet years (1982, 1986, 1989, and 1992) and four dry years (1984, 1985, 1987, and 1993) are chosen for the composite analysis. Fig. 3a shows the wet minus dry composite of SSTs. The composite is characterized by a strong positive SST anomaly pattern over the central and eastern equatorial Pacific Ocean and a negative SST anomaly pattern over the western Pacific Ocean, which is a typical SST anomaly distribution during mature El Niño years. This suggests that El Niño events in their mature phase are closely related to positive anomalies of precipitation over Tanzania during the short-rains season. Strong, warm SST anomalies are observed over the western Indian Ocean, while cold SST anomalies occur over the eastern Indian Ocean. Over the Atlantic Ocean, cold SST anomalies are located over the tropical regions, and warm SST anomalies are found in the extratropical regions. For all the four wet years used in the composite analysis, the SST anomaly patterns over the Indian Ocean and the Atlantic Ocean are similar to those in Fig. 3a. In contrast, all the four dry years used in the composite SST analysis are characterized by opposite anomalies over the Indian Ocean and the Atlantic Ocean. However, only two wet years (i.e., 1982 and 1986) exhibit the SST anomaly pattern over the Pacific Ocean similar to that in Fig. 3a, and two dry years (i.e., 1984 and 1985) show the SST anomaly pattern nearly opposite to that in Fig. 3a. It is therefore apparent that the SST anomalies over the Indian Ocean and the Atlantic Ocean play an important role in determining the interannual variability of precipitation for Tanzania.

Although the subtropical highs over the Indian Ocean and Atlantic Ocean are mostly outside our inner domain, they strongly influence the flow over eastern Africa. On the basis of 12-year NCEP (National Centers for Environmental Prediction)/NCAR reanalysis we found that the centers of the St. Helena High, the subtropical high over the northern Atlantic Ocean, the Mascarene High, and the Arabian High during the months of October, November, and December are located at 10°W, 27.5°S; 37.5°W, 28°N; 70°E, 27.7°S; and 51°E, 22.5°N. Fig. 4a shows the wet minus dry composites of geopotential height and meridional wind at 850 mbar based on the NCEP/NCAR reanalysis. Stronger St. Helena High and the subtropical high over northern Atlantic Ocean, a weaker Mascarene High, and a southward movement of the Arabian High are clearly evident. The southward shift of the Arabian High may cause an earlier advance of the northeast monsoons into Tanzania, while the weakened Mascarene High results in weaker southeast monsoons. The net result is that the zonal component of the ITCZ shifts farther south and causes an early onset of the rainy season over Tanzania. As shown in Fig. 5, the northerly wind along the Tanzania coast and the Indian Ocean indicates that northerly wind is stronger in the wet years than the dry years, and the ITCZ moves farther south. The rainy

Table 3. N is the Number of Days With Observed Precipitation Data From October to December, r is Correction Coefficient Between Simulated and Observed Daily Precipitation, and r_c is Critical Correction Coefficient at 1% Significance Level Represented on the Basis of Student's t-Tests

	1982	1983	1984	1985	1986	1987	1988	1989	1990	1991	1992	1993
N	39	45	63	49	67	54	62	62	57	53	22	28
r	0.57	0.44	0.42	0.47	0.55	0.44	0.61	0.40	0.13	0.61	0.50	0.52
r_c	0.41	0.39	0.33	0.37	0.32	0.35	0.33	0.33	0.34	0.36	0.51	0.46

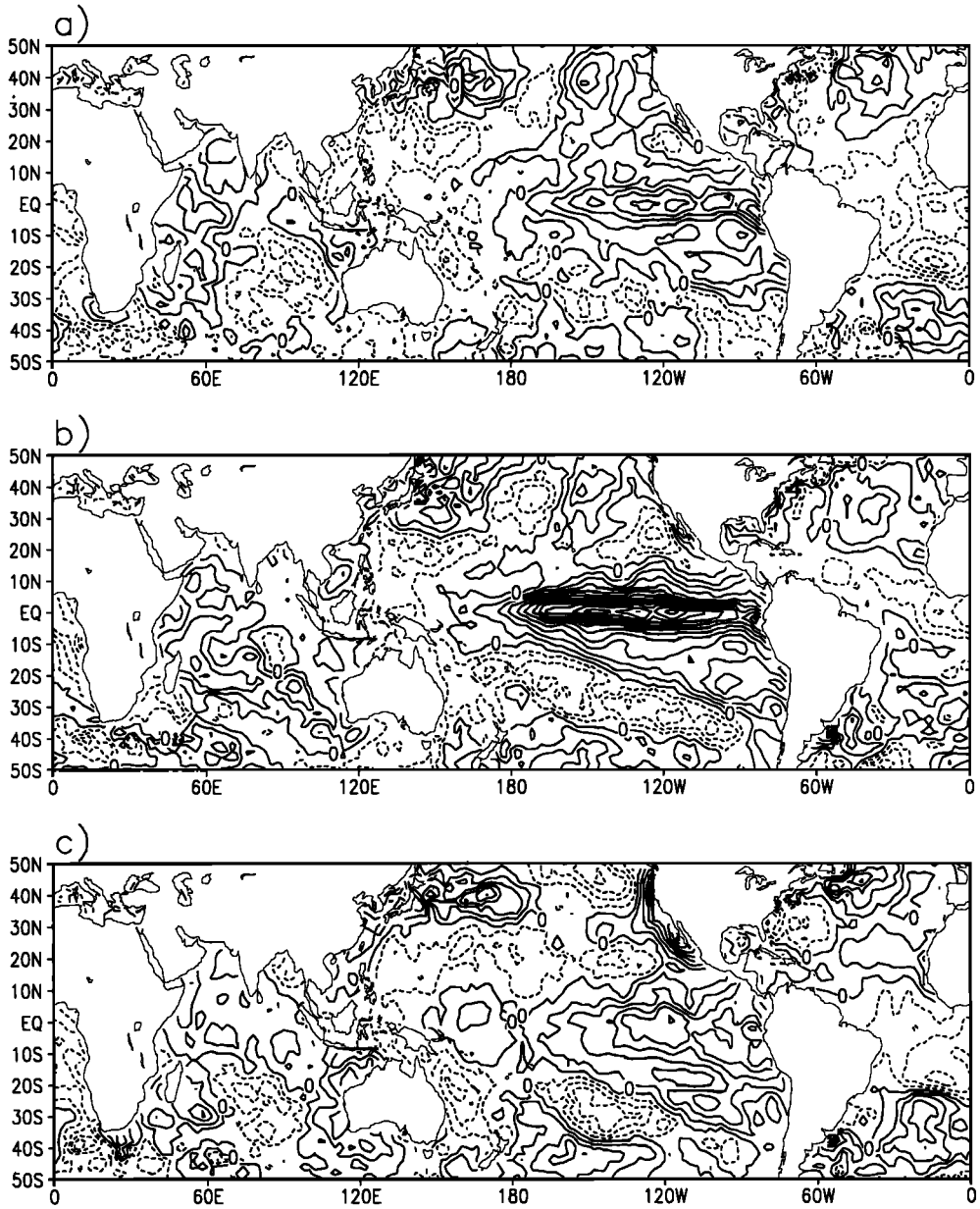

Figure 3. Wet composite minus dry composite, averaged over the months of October–December, for observed SST (in degrees Kelvin) for (a) Tanzania, (b) Lake Victoria, (c) western Kenya Highlands, (d) eastern Kenya Highlands, and (e) Turkana channel. Contour internal is 0.2° and the reference "0" contour is labeled. The broken/solid lines represent negative/positive contours.

season came earlier in 1982 and 1986 due to the southward shift of the Arabian High and the weakness of the Mascarane High. The enhanced St. Helena High intensifies the moist westerly flow over the Angola plateau and extends it farther east. The weaker Mascarane High results in the weaker easterly flow to central Tanzania from the Indian Ocean (not shown). The net result is that the meridional ITCZ is shifted farther east into Tanzania, and the corresponding zonal convergence over Tanzania intensifies. All the four wet years are associated with an intensified St. Helena High and a weaker Mascarane High.

2.2. Lake Victoria

There are 33 model grid points on Lake Victoria. Strong mesoscale circulation (i.e., lake breeze) characterized by an intense diurnal cycle in precipitation over Lake Victoria was discussed by *Sun et al.* [this issue]. The mesoscale circulation is not captured in the ECMWF data due to its coarse resolution. Consequently, the ECMWF data are not suitable for validation of the model-simulated circulation. No observed precipitation data over Lake Victoria is available for this study. However, previous investigations indicate that there is a strong positive correlation between the lake level and the monthly precipitation over the Lake Victoria catchment [*Morth*, 1967]. Recently, *Birkett* [1997] has analyzed the evolution of the lake level during 1992 and 1993. The decrease of the lake level during both the short rains season imply a reduction in precipitation during the short rains of 1992 and 1993. Fig. 6 shows the simulated precipitation anomalies from the simulated 12-year mean. The strong negative precipitation anomaly in 1993 and

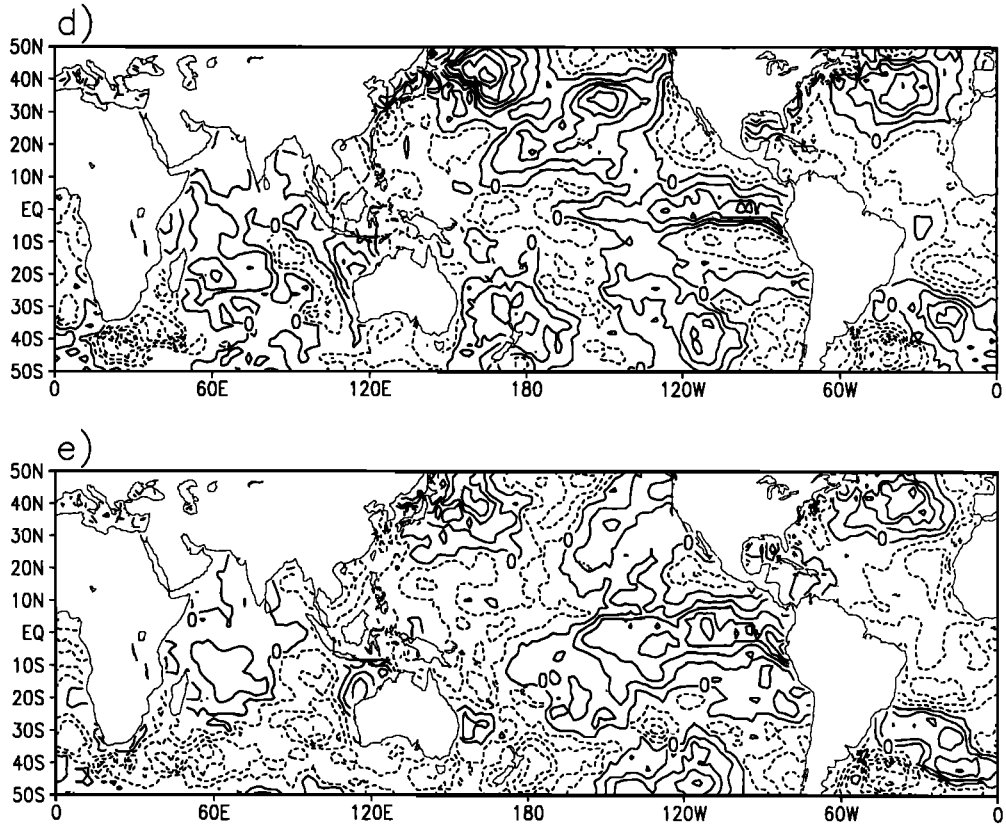

Figure 3. (continued)

the weak negative precipitation anomaly in 1992 during short rains are in good agreement with the observations of the lake level. We note that there are three El Niño events and one La Niña event during the 12-year simulation (i.e., 1982/1983, 1986/1987, and 1991/1992). *Ogallo* [1988] investigated the relationships between the seasonal rainfall over East Africa and the southern Oscillation for the period 1923–1984 and indicated significant negative zero lag correlations between the Southern Oscillation Index (SOI) and the seasonal rainfall over the Lake Victoria catchment during the short-rains season. This suggests that rainfall higher (lower) than the long-term mean over the Lake Victoria catchment was evident during the El Niño (La Niña) years. The Lake Victoria catchment is the region surrounding the lake. Thus we may assume that the rainfall over Lake Victoria is also negatively correlated to the SOI. The simulated positive precipitation anomalies in 1982, 1986, and 1991 and negative precipitation anomaly in 1988 during the short-rains season suggest that there is a good likelihood that the model simulation in ENSO years is correct. Composite analysis also suggests that precipitation over the Lake Victoria catchment decreases during the short rains in the year prior to the mature phase of El Niño events (A. W. Majugu, personal communication, 1996). Simulated precipitation deficits in 1985 and 1990 suggest that the model simulation in these two years may be realistic. Overall, there is thus some evidence that the model reproduced the interannual variability of precipitation.

Four wet years (1982, 1986, 1989, and 1991) and four dry years (1985, 1988, 1992, and 1993) are chosen for the composite analysis. Fig. 3b shows the wet minus dry composite of SST. Strong positive SST anomalies over the central and eastern equatorial Pacific Ocean and negative SST anomalies over the western Pacific Ocean are clearly evident. Warm SST anomalies over most of the Indian Ocean and the subtropical regions of the Atlantic Ocean and cold SST anomalies along the Angola coast are also evident. This suggests that some of the precipitation variability is associated with the El Niño events. However, some of the wet and dry episodes are not related to the ENSO events (e.g., 1989 and 1993). Wet conditions in 1989 are associated with warm SST anomalies over the western Indian Ocean, subtropical South Atlantic Ocean, and cold SST anomalies along the southern Atlantic coast region, which is similar to the SST anomaly patterns over the Indian and Atlantic Oceans in Fig. 3b. Dry conditions in 1993 are associated with cold SST anomalies over the western Indian Ocean and warm SST anomalies over the Atlantic Ocean between 10°N and 30°S, which is almost opposite to the SST anomaly patterns over the Indian and Atlantic Oceans in Fig. 3b. Both the ENSO-related and the non-ENSO-related wet and dry conditions over most of East Africa are associated with the SST anomaly patterns over the Indian Ocean and the Atlantic Ocean shown in Fig. 3b. We postulated that the precipitation fluctuations over Lake Victoria may be more directly a response to SST fluctuations over the Indian Oceans and the Atlantic Ocean, although these SST fluctuations themselves may be related to ENSO events.

Fig. 4b shows the wet minus dry composite of geopotential height at 850 mbar based on the NCEP/NCAR reanalysis. The St. Helena High, the Arabian High, and the Mascarene High are shifted equatorward. The equatorward shift of the St. Helena High tends to intensify the low-level westerly flow over the Congo Basin and extend it to Lake Victoria (Fig. 7), while the equatorward shift of the Arabian High and the Mascarene

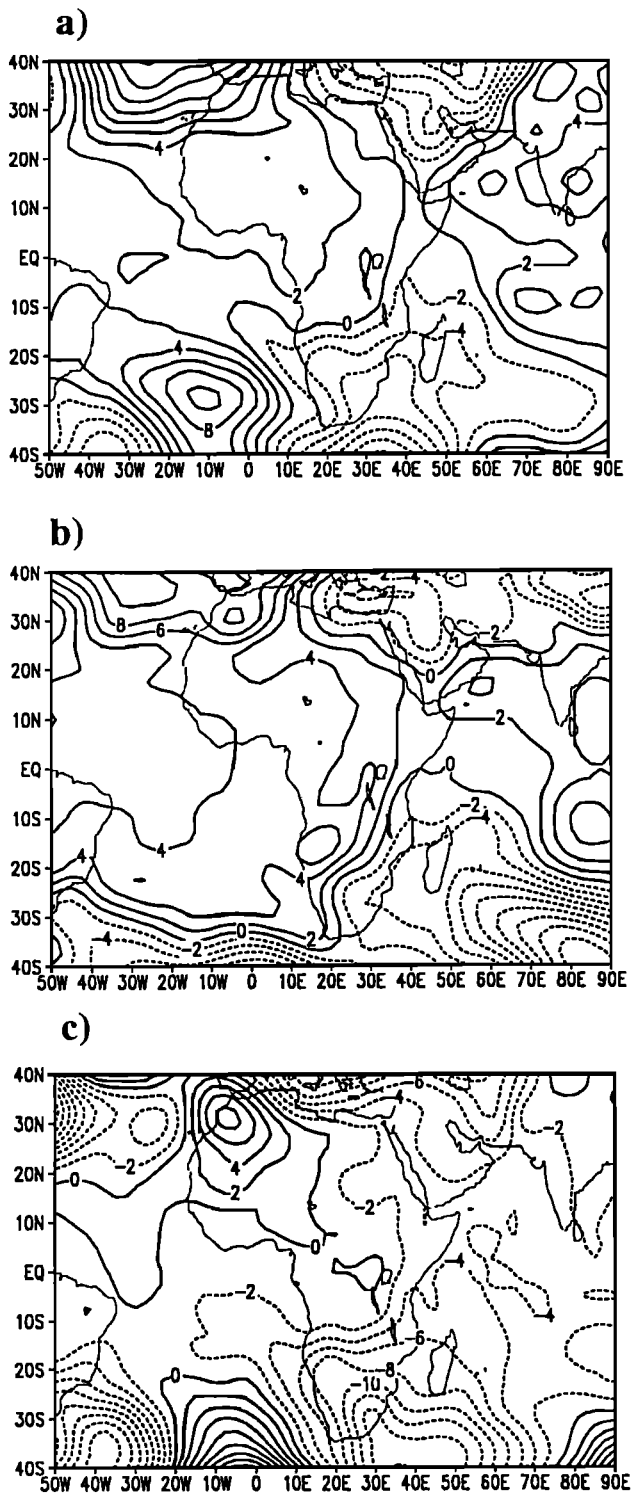

Figure 4. Same as Fig. 3 except for NCEP/NCAR geopotential height (m) reanalysis at 850 mbar.

High lead to mainly easterly flow toward Lake Victoria from the Indian Ocean. Note that both the northeast monsoons and the southeast monsoons are thermally stable and associated with subsiding air, while the easterly flow from the equatorial Indian Ocean is thermally unstable and associated with the ITCZ over the Indian Ocean. The moist westerly flow from the Atlantic Ocean and the moist easterly flow from the Indian Ocean converge over Lake Victoria and result in an abnormal

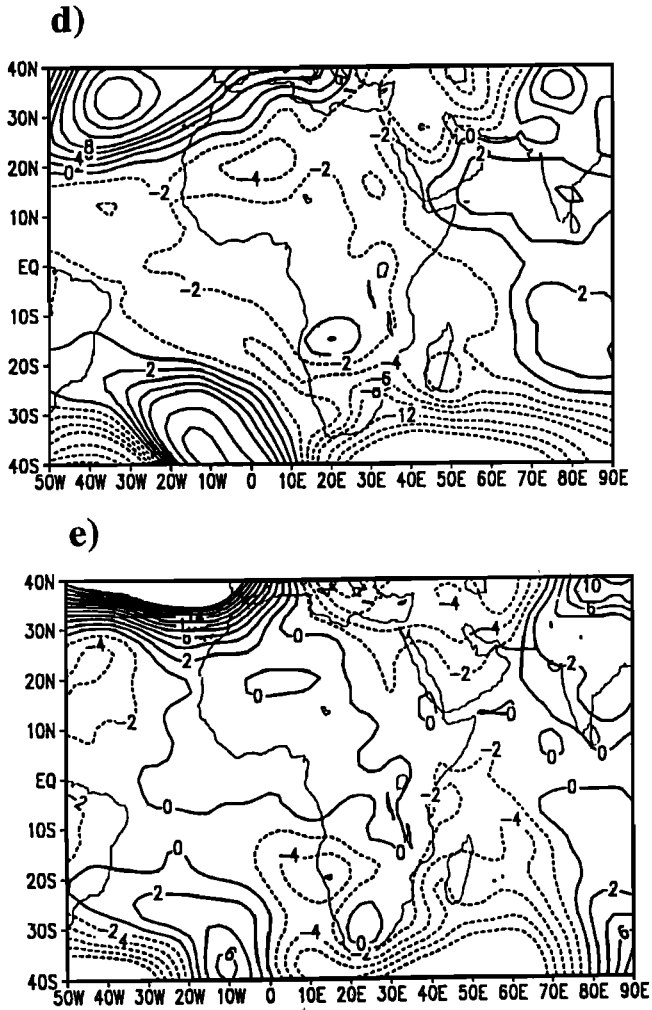

Figure 4a. (continued)

upward motion over Lake Victoria (Fig. 7), which favors precipitation formation over Lake Victoria.

2.3. Kenya Highlands

The region of Kenya Highlands experiences its precipitation peak during the short rains. It is feasible to treat the Kenya Highlands as one region to validate the simulated precipitation

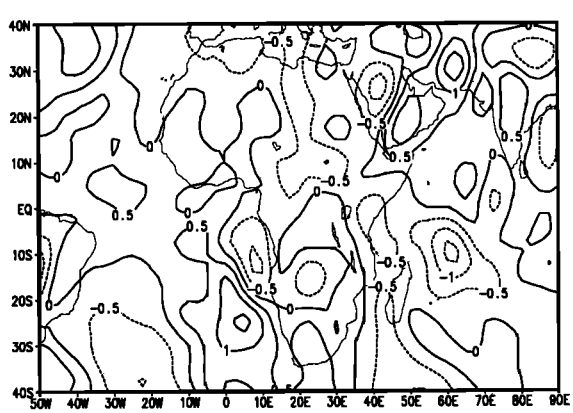

Figure 5. Same as Fig. 3a except for the observed meridional wind at 850 mbar. Units are in m/s.

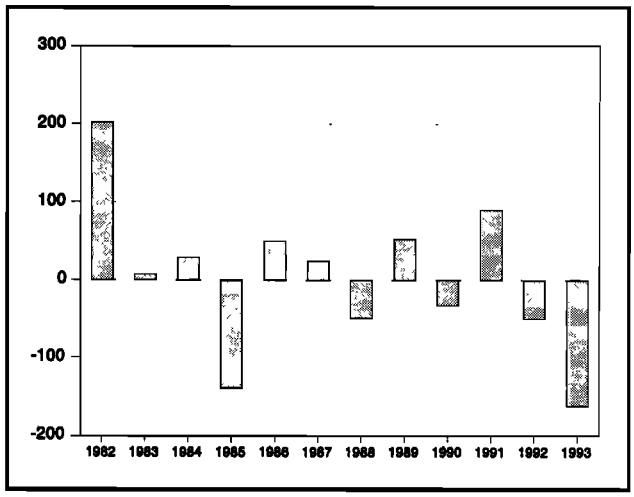

Figure 6. Simulated precipitation anomalies from the 12-year simulated mean over Lake Victoria for the October to December season. Units are in millimeters.

for 1 month or one season. However, the Kenya Highlands is not a homogeneous region for precipitation. *Ininda* [1994] divided the Kenya Highlands into four subregions due to the complex terrain of the region. In order to validate the model performance in reproducing the interannual variability in precipitation regimes, the averaging of precipitation should be carried out separately for each homogeneous region. There are two precipitation maxima located at each side of the peak of the Kenya Highlands. We divide the Kenya Highlands into two subregions because of the limitation of the model horizontal resolution: western Kenya Highlands (WKH) and eastern Kenya Highlands (EKH). WKH is the Lake Victoria side of the Kenya Highlands, and EKH is the Indian Ocean side of the Kenya Highlands. Each of the WKH and EKH regions includes 16 model grid points. Lake Victoria may play a role in modulating the precipitation variations of the WKH subregion, while the Indian Ocean influences the precipitation variations of the EKH subregion directly. The precipitation is mainly concentrated in October and November for both the WKH and the EKH subregions during the short rains. The precipitation zone migrates out of the Kenya Highlands in December in response to the southward movement of the ITCZ. Only an isolated precipitation maximum appears to persist near the town of Embu in Kenya due to local terrain effects. Therefore our analysis is based on the October–November average.

A total of 96 and 46 stations were available for the WKH and EKH regions, respectively. The 12-year observed mean precipitation for the WKH and EKH regions are 219.3 and 351.0 mm, respectively. The simulated 12-year mean precipitation for the WKH and EKH regions are 289.5 and 281.3 mm, respectively. In our model the presence of tropical forests over the WKH region and semiarid and desert types of land use over the EKH region may not represent the actual land use properly [see *Sun et al.*, this issue, Figure 1]. The inaccurate description of the land use may partly contribute to the relatively high simulated precipitation over the WKH region and low precipitation over the EKH region. An additional contribution to the discrepancy between observed and simulated precipitation is likely given by the relative smoothness of the model topography.

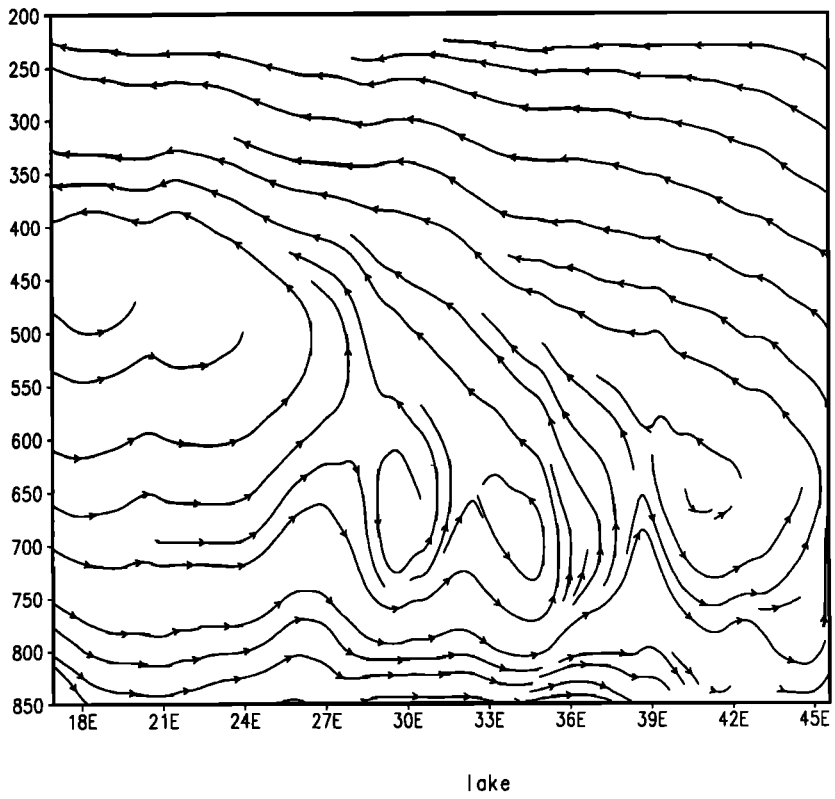

Figure 7. Wet composite minus dry composite of simulated zonal-vertical circulation (U, W), averaged from 3.2°S to the equator, and October to December.

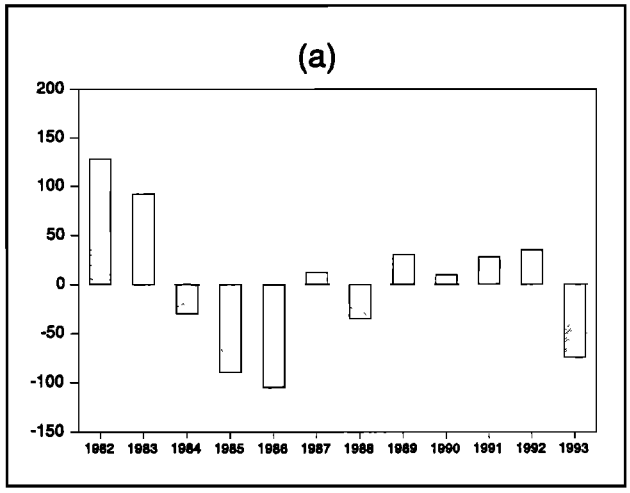

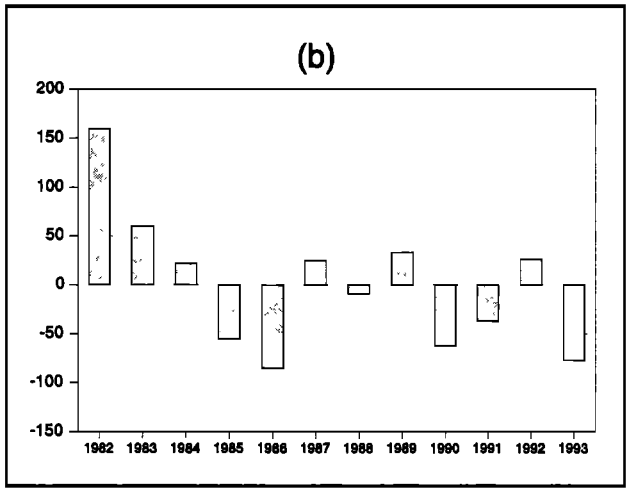

Figure 8. Same as Fig. 2 except for the western Kenya Highlands.

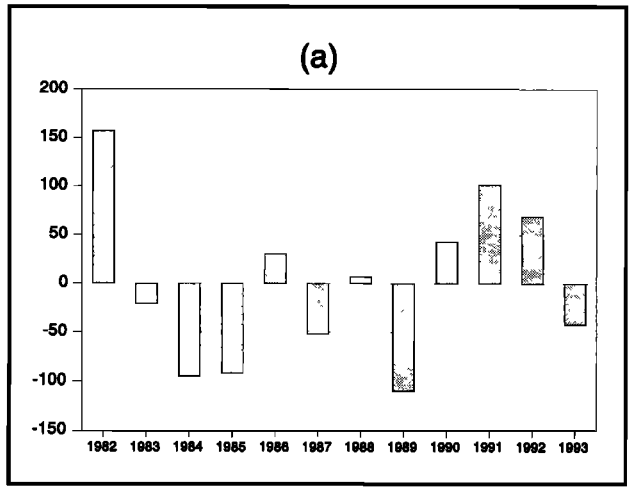

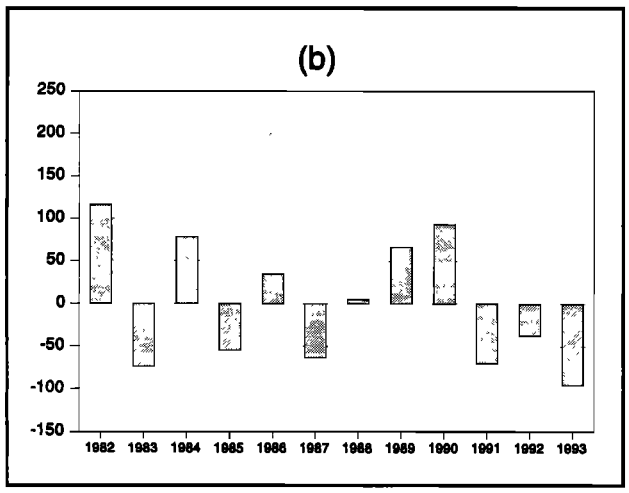

Figure 9. Same as Fig. 2 except for the eastern Kenya Highlands.

Figures 8 and 9 show the simulated precipitation anomalies from the simulated 12-year mean and the observed precipitation anomalies from the observed 12-year mean for the WKH and EKH regions, respectively. The correlation coefficient r between the simulated precipitation anomalies and the observed precipitation anomalies is 0.847 over the WKH region and 0.455 over the EKH region. This result indicates that the simulated and observed precipitation anomalies are significantly (not significantly) correlated at the 1% significance level during the 12-year simulation for the WKH (EKH) region. Precipitation over the EKH region is mainly attributed to the orographic uplifting processes. As discussed in section 5.3 of the companion paper [*Sun et al.*, this issue], the inaccurate SSTs in the model may result in the weaker low-level easterly winds over the Kenya coast in the model simulation, which may be largely responsible for the precipitation deficit over the KH region in 1988. We also found the inconsistency of the SSTs near the Kenya coast between the SST data set [*Shea et al.*, 1992] we used and the SST data set. This may cause the poor performance in simulating precipitation over the EKH region. The inconsistency of the interannual variability of precipitation between the WKH and the EKH regions suggests that different factors control the precipitation variability for these two regions. The model reproduces the wet conditions in 1982, 1983, 1987, 1989, and 1992 and the dry conditions in 1985, 1986, 1988, and 1993 for the WKH region and wet conditions in 1982, 1986, 1988, and 1990 and dry conditions in 1983, 1985, 1987, and 1993 for the EKH region. However, the model fails to reproduce the wet conditions in 1984 for the WKH region, 1984 and 1989 for the EKH region, and the dry conditions in 1990 and 1991 for the WKH region, and 1991 and 1992 for the EKH region.

Four wet years (1982, 1983, 1989, and 1992) and four dry years (1985, 1986, 1988, and 1993) for the WKH region are chosen for the composite analysis. Fig. 3c shows the wet minus dry composite of SST for the WKH region. Positive SST anomalies over the central and eastern equatorial Pacific Ocean and negative SST anomalies over the western Pacific Ocean are observed. Warm SST anomalies over the northern Indian Ocean, and the extratropical regions of the Atlantic Ocean, and cold SST anomalies over the tropical Atlantic Ocean are also presented. The SST anomaly pattern in Fig. 3c is similar to that for Lake Victoria in Fig. 3b. This may imply that the interannual variability of precipitation over Lake Victoria and the WKH subregion are strongly coupled. Note that the composites shared five out of eight of the same years for the WKH and LV regions. Compared to Fig. 3b, in Fig. 3c the warm SST anomalies are much weaker over the central and eastern equa-

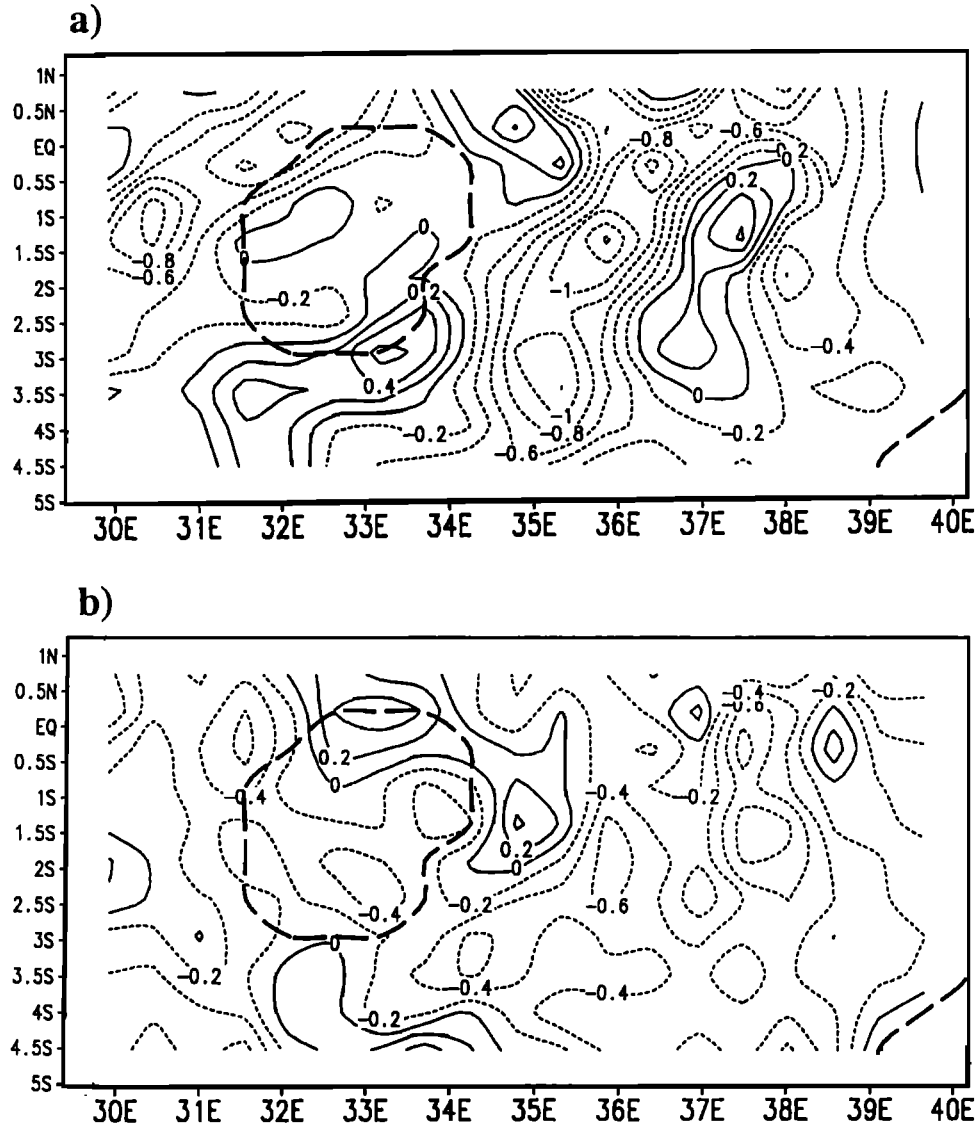

Figure 10. Wet composite minus dry composite of simulated momentum convergence at 850 mbar averaged over the months of October–November (noon simulation) for (a) western Kenya Highlands and (b) eastern Kenya Highlands. Unit is 10^{-5} s^{-1}.

torial Pacific Ocean, the warm SST anomalies are stronger and farther away from the equator over the southern Atlantic Ocean, and the cold SST anomalies over the southern Indian Ocean extend farther north. These differences indicate that some large-scale factors are different regarding the mechanisms that control the precipitation variability over Lake Victoria and the WKH subregion. As an example, a positive anomaly pattern of precipitation over Lake Victoria is observed in the three El Niño years during the 12-year simulation, while only a positive anomaly pattern of precipitation over the WKH region is observed in one El Niño year (i.e., 1982), and a negative precipitation anomaly dominates in the other two El Niño years (i.e., 1986 and 1991).

Usually, southeast monsoons prevail during most of October, and northeast monsoons prevail during November over the WKH region. Weaker Arabian High and weaker Mascarene High in Fig. 4c lead to weaker northeast monsoons and southeast monsoons, respectively. This results in weaker low-level large-scale divergence over the WKH region, which enhances the development of convection. Precipitation over the WKH region mainly occurs during the daytime due to the lake breeze. Fig. 10a shows the wet minus dry composite of convergence at 850 mbar at noontime. The low-level convergence anomalies over the WKH region associated with weaker Arabian High and Mascarene High account for the positive precipitation anomalies in the wet minus dry composite.

The model produced a correct sign of the precipitation anomalies in most years over the EKH region, although the correlation between the simulation and the observations was not significant at the 1% significance level. The four wet years (1982, 1986, 1988, and 1990) and the four dry years (1983, 1985, 1987, and 1993) are chosen for the composite analysis over the EKH region. Fig. 3d shows the wet minus dry composite of SST for the EKH region. The El Niño-related SST anomaly pattern disappears, which suggests that the interannual variability of precipitation is not directly related to the El Niño events. The SST anomaly pattern over the Atlantic Ocean is similar to that over the WKH region, with warm SST

Table 4. Details of Precipitation Stations Over Turkana Channel

Station	Latitude, °N	Longitude, °E	Elevation, m
Lokori South Turkana	1.57	36.02	820
Buna Police Post	2.48	39.01	656
Kekorongo Irrigation Scheme	2.53	35.25	820
North Horr Police Post	3.19	37.04	
Oropoi Police Post	3.48	34.21	984
Lokitaung D.O.'S office	4.15	35.45	787
Kaleng Trading Center	4.23	35.33	787
Kokoro Police Post	4.40	35.43	656

anomalies over the western Indian Ocean and, especially, along the East African coast.

Fig. 4d shows the wet minus dry composite of geopotential height at 850 mbar based on the NCEP/NCAR reanalysis for the EKH region. The Mascarene High is greatly weakened, and the Arabian High shifts equatorward. Thus the southeast monsoons recede earlier over the EKH region, and the northeast monsoons prevail over the EKH region during most of October and November. The equatorward shift of the Arabian High leads to mainly easterly flow over the EKH region. This easterly flow, originated from the ITCZ over the Indian Ocean, is thermally unstable and brings more water vapor to the Kenya Highlands. This moisture easterly flow leads to an increase in precipitation over the windward slope of the Kenya Highlands (i.e., EKH) due to orographic uplifting. As shown in Fig. 10b, the low-level convergence anomalies over the EKH region are associated with the thermally unstable easterly flow and tend to enhance convective precipitation.

2.4. Turkana Channel

The Turkana channel lies between the Ethiopian highlands and the East African highlands, which includes 39 model grid points. Strong winds (i.e., the Turkana low-level jet) exist throughout the channel, and divergence is a predominant feature [*Kinuthia*, 1992]. The Turkana Channel is a semiarid region. As shown by *Sun et al.* [this issue], the model mostly reproduced the Turkana low-level jet, while due to their coarse resolutions, both the ECMWF data set and the NCEP/NCAR reanalysis did not capture the jet. Consequently, the ECMWF data and NCEP/NCAR reanalysis are not suitable for validation of the model performance. The precipitation stations available for this study over the Turkana channel are listed in Table 4. The eight-station, 12-year mean observed precipitation for the short rains is 55.5 mm. The corresponding simulated precipitation is 70.0 mm, which was obtained by first interpolating to the station locations listed in Table 4 and then averaging the interpolated values. The model simulation is wetter than the observations. Observations show precipitation maxima over the highlands and minima at the bottom of the channel, corresponding to steep gradients in local terrain. The relatively lower gradients of the highlands and shallower vertical extent of the Turkana channel in the model increase the channel width, which results in a weakened simulated low-level jet and a reduction in the precipitation gradient between the highlands and the bottom of the channel.

Figure 11 shows the simulated precipitation anomalies from the 12-year simulated mean and the observed precipitation anomalies from the 12-year observed mean. The correlation coefficient r between the simulated precipitation anomalies

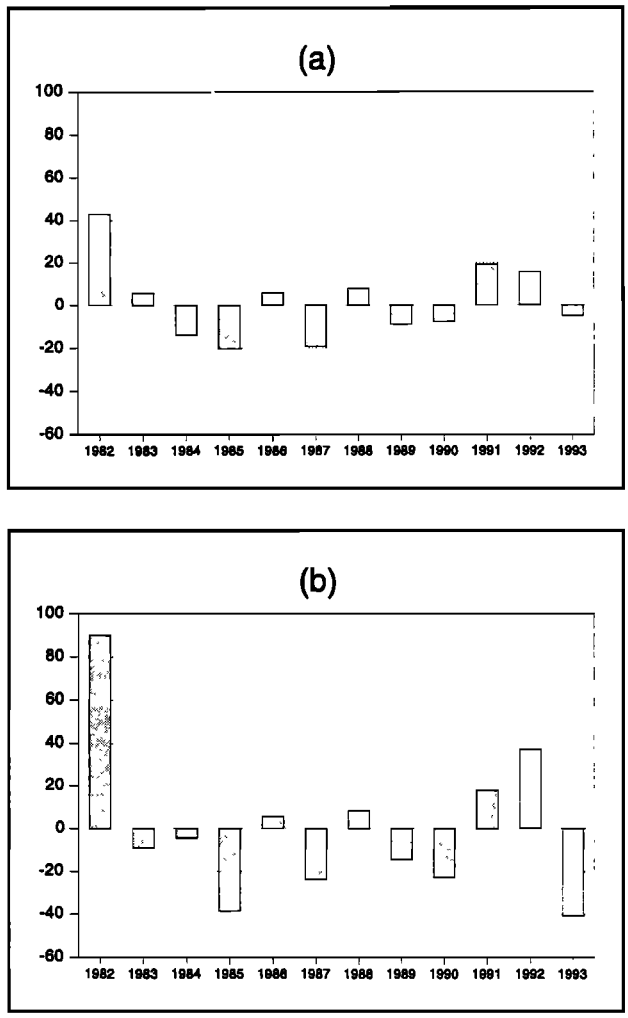

Figure 11. Same as Fig. 2 except for the Turkana channel.

and the observed precipitation anomalies is 0.906, which is larger than the critical correlation coefficient 0.708 for the 1% significance level. Therefore the simulated and observed precipitation anomalies are significantly correlated at 1% significance level for the 12 years. The observed wet conditions in 1982, 1986, 1988, 1991, and 1992 and the dry conditions in 1984, 1985, 1987, 1989, 1990, and 1993 are successfully reproduced in the model simulation. The model produces a weaker positive precipitation anomaly in 1983 instead of the observed dry conditions. Overall, the interannual variability of precipitation is generally captured by the model. However, the modeled interannual variability of precipitation is less than the observed variability, i.e., the anomalies are mostly the correct sign but are smaller than observations. For example, the severe dry conditions in 1993 are largely reduced in the model simulation.

Because of the strong divergence associated with the Turkana low-level jet, convective precipitation over the Turkana channel is very small. The limited amount of convective precipitation is mainly concentrated during nighttime perhaps due to the mountain-valley circulations over the channel. The nonconvective precipitation is the dominant component of the total precipitation over the Turkana channel and accounts for 85% of the total precipitation amount in the 12-year simulation. On the basis of spectral analysis we also found that pre-

cipitation exhibits variations with 4–8 day periods for the 12-year simulation, which may be associated with the propagation of easterly waves originated from the Indian Ocean.

Four wet years (1982, 1988, 1991, and 1992) and four dry years (1984, 1985, 1987, and 1989) are chosen for the composite analysis. The changes in total precipitation, large-scale precipitation, and convective precipitation are 36.0, 29.2, and 6.8 mm in the wet minus the dry composites, respectively. This result suggests that interannual changes in circulation systems play an important role for the interannual variability of precipitation.

Fig. 3e shows the wet minus dry composite of SST for the Turkana channel. Strong positive SST anomalies over the central and eastern equatorial Pacific Ocean and negative SST anomaly over the western Pacific Ocean are well depicted. This result suggests that the precipitation variability is strongly associated with El Niño events, which is consistent with *Ogallo* [1988]. However, some of the wet episodes are not related to the El Niño events. As an example, 1988 was a typical La Niña year, and the positive precipitation anomalies during that year may be related to the warm SST anomalies along the East African coast, which contributes to more water vapor transport from the Indian Ocean to the Turkana channel. The cold SST anomalies over the tropics and warm SST anomalies over the extratropics in the Atlantic Ocean are also present in Fig. 3e.

Fig. 4e shows the wet minus dry composite of geopotential height at 850 mbar based on the NCEP/NCAR reanalysis. Both the Arabian High and the Mascarene High are weaker and shift eastward compared to averaged conditions. The trade inversion associated with the subtropical highs over the Indian Ocean is best developed on the eastern equatorward side of the subtropical highs and weakens broadly following the trade wind airstream equatorward and toward the western part of the Indian Ocean [*Hastenrath*, 1991]. The weakness and eastward shift of both the Arabian High and the Mascarene High tend to weaken the trade inversion over the equatorial Indian Ocean and East African coast and suggests wider thermal unstable zone over the equatorial Indian Ocean, which is favorite for the formation of easterly waves. The weaker Arabian High and weaker Mascarene High suppress the wind speed at the entrance of the Turkana channel and, consequently, result in a weakened Turkana low-level jet and low-level divergence. As shown in Fig. 12, wind speed is lower in the wet composite than in the dry composite. The eastward shift of the Arabian High and the Mascarene High lead to mainly easterly flow over East Africa, with marked injection of moisture into East Africa from the Indian Ocean. Overall, weaker divergence and more moisture over the Turkana channel account for the increase of precipitation in the wet minus dry composite of precipitation.

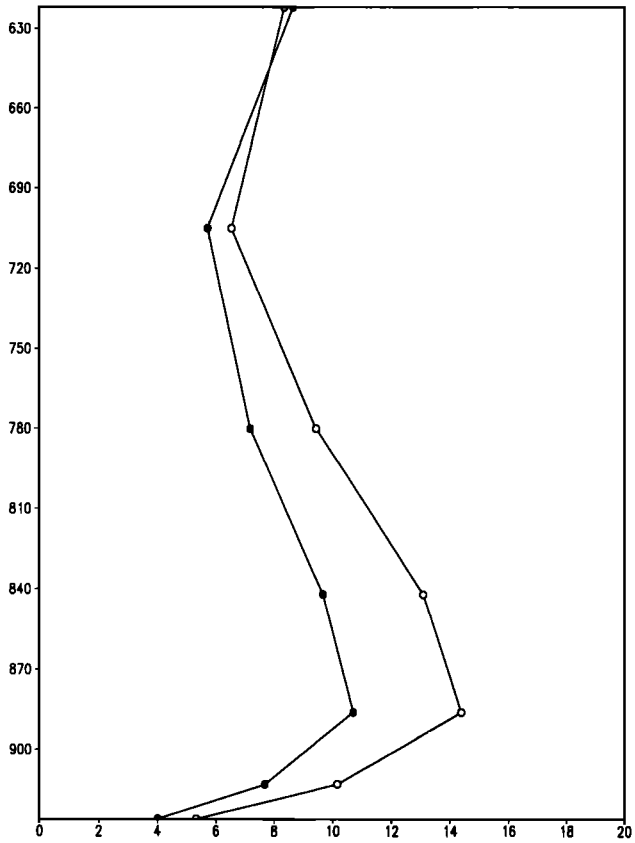

Figure 12. Simulated vertical profiles for horizontal wind speed (m/s). Solid circle, wet composite; open circle, dry composite.

3. Conclusions

We have employed the NCAR RegCM2 to simulate the interannual variability of precipitation over eastern Africa during the short rains seasons by performing simulations for the years 1982–1993. The model reproduced the observed interannual variability of precipitation in most of the years. Composites, based on wet and dry year analysis, were constructed to investigate the possible reasons for the precipitation variability.

El Niño events in their mature phase are closely related to the positive precipitation anomalies over Tanzania during the short rains. However, the SST anomalies over the Indian Ocean and the Atlantic Ocean may play a more important role in determining the interannual variability of precipitation for Tanzania. Strong warm SST anomalies are observed over the western Indian Ocean, while cold SST anomalies are observed over the eastern Indian Ocean in the wet minus dry composite. For the Atlantic Ocean, cold SST anomalies over the tropical regions and warm SST anomalies over the extratropical regions dominate in the wet minus dry composite. The southward shift of the Arabian High and weaker Mascarene High may result in southward shift of the zonal component of the ITCZ, and they are responsible for the earlier onset of rainy season in 1982 and 1986. The stronger St. Helena High and weaker Mascarene High lead to eastward shift of the meridional branch of the ITCZ for the wet years.

Observed lake level data and work described in previous papers were used to validate the model simulations over Lake Victoria. The strong connection between the interannual variability of precipitation over Lake Victoria and the ENSO events observed in previous studies was confirmed by the model simulations. The precipitation fluctuations, especially for wet years, are influenced by SST anomalies over the Indian Ocean and the Atlantic Ocean. The equatorward shift of the St. Helena High tends to enhance the low-level moist westerly flow over the Congo Basin and extend it to Lake Victoria, and the equatorward shift of the Arabian High and the Mascarene High lead to mainly easterly flow over the equatorial Indian Ocean during wet years. The moist westerly flow from the Atlantic Ocean and the moist easterly flow from the Indian Ocean converge over Lake Victoria, which account for the

increase in precipitation over Lake Victoria in the wet minus dry composite.

The model produced the correct sign of the interannual variability of precipitation over the western part (WKH) and eastern part (EKH) of the Kenya Highlands in all the years except for 1984, 1990, and 1991 over the WKH region and 1984, 1989, 1991, and 1992 over the EKH region. The interannual variability of precipitation over Lake Victoria and the WKH subregion are strongly coupled. Positive precipitation anomalies are usually associated with weaker Arabian High and Mascarene High, which weaken the large-scale divergence over the WKH region and favor the development of convection. The interannual variability of precipitation over EKH is not directly related to the El Niño events. Wet conditions over the EKH region are usually associated with warm SST anomalies over the western Indian Ocean. The equatorward shift of the Arabian High leads to mainly easterly flow over the EKH region, which carries enhanced water vapor and induces an increase in precipitation by orographic lifting.

The model produced slightly wetter conditions over the Turkana channel compared to the observations. Higher model resolution is required to simulate the steep gradients in precipitation associated with the topographic gradients around the channel. Composite analysis indicates a strong El Niño signal for the wet years, associated with warm SST anomalies over the Indian Ocean and more active easterly waves which propagate into the Turkana channel and lead to increased precipitation. Also, the weaker Arabian High and Mascarene High suppress the wind speed at the entrance of the Turkana channel and, consequently, result in a weakened Turkana low-level jet.

The same initial soil conditions are applied to each year's simulation. That the model produces the interannual variability of precipitation in most of the years may suggest that the external factors play an important role in determining the precipitation anomalies for the short-rains season. Therefore the global forecasts for large-scale circulations and SSTs will be used to drive the lateral boundary conditions for the RegCM2 for the development of the Seasonal Climate Prediction System (SCPS) for eastern Africa.

Acknowledgments. This research was supported by the NSF/Climate Dynamics Program, project ATM-9424289. We extend our gratitude to G. Bates and C. Shields who helped in using RegCM2. M. Indeje, Y. Song, and G. Pouliot made many contributions in the work reported in this paper. We acknowledge the enlightening discussions with L. Xie, R. Burton, C. Basalirwa, A. Majugu, N. Pyuzza, G. Obua, and P. Ambenje for their help during the various stages of this work. Some of the precipitation data were obtained from the Drought Monitoring Center, Nairobi, and their assistance is deeply appreciated. The model integrations were performed on the North Carolina Supercomputing Center on the T90 supercomputer. The postprocessing of the model output was carried out at the *FOAM*^{V} Visualization and Parallel Computing Facility, at North Carolina State University. *FOAM*^{V} is supported by the IBM Environmental Research Program (ERP). Any opinions, findings, conclusions, or recommendations expressed in this material are those of the authors and do not necessarily reflect the views of the IBM Corporation. One of the authors, LO, was supported by the START program and their support is greatly appreciated.

References

Anyamba, K. E., On the monthly mean lower tropospheric circulation and the anomalous circulation during the 1961/62 floods in East Africa, M.S. thesis, Dep. of Meteorol., Univ. of Nairobi, Kenya, 1984.

Anyamba, K. E., and L. J. Ogallo, Anomalies in the windfield over East Africa during the East African rainy season of 1983/84, in *Proceedings of the First WMO Workshop on Diagnosis and Prediction of Monthly and Seasonal Atmospheric Variations Over the Global, Long-Range Forecasting, Res. Rep. Ser. 6, WMO/TD. 87*, pp. 128–133, World Meteorol. Organ., Geneva, 1985.

Beltrando, G., Space-time variability of rainfall in April–November over East Africa during the period 1932–1983, *Int. J. Clim., 10*, 691–702, 1990.

Birkett, C., A new global lake and catchment conservation database, in *IDEAL Bulletin*, 4 pp., IDEAL Program, Wis., Madison, 1997.

Davis, T. D., C. E. Vincent, and A. K. C. Beresford, July–August rainfall in west-central Kenya, *J. Clim., 5*, 17–33, 1985.

Farmer, G., Seasonal forecasting of the Kenya coast short rains, 1901–84, *J. Clim., 8*, 489–497, 1988.

Flohn, H., East African rains of 1961/62 and the abrupt change of the White Nile discharge, *Paleoecol. Afr. Surround. Isl., 18*, 3–18, 1987.

Hastenrath, S., *Climate Dynamics of the Tropics*, Kluwer Acad., 488 pp., Norwell, Mass., 1991.

Hastenrath, S., A. Nicklis, and L. Greischar, Atmospheric mechanisms of climate anomalies in the western equatorial Indian Ocean, *J. Geophys. Res., 98*, 20,210–20,235, 1993.

Ininda, J. M., Numerical simulation of the influence of the sea surface temperature anomalies on the East African seasonal rainfall, Ph.D. thesis, Univ. of Nairobi, Kenya, 1994.

Johnson, D. H., and H. T. Morth, Forecasting research in East Africa, in *Tropical Meteorology in Africa*, edited by D. J. Bargman, pp. 56–137, Munitalp, Nairobi, 1960.

Kiangi, P. M. R., and J. J. Temu, Equatorial westerlies in Kenya, Are they always rain-laden?, *Proceedings of the WMO Regional Scientific Conference on GATE*, pp. 144–146, WAMEX and Trop. Meteorol., Dakar, Senegal, 1984.

Kinuthia, J. H., Horizontal and vertical structure of the Lake Turkana jet, *Mon. Weather Rev., 120*, 1248–1274, 1992.

Minja, W. E. S., A comparative investigation of weather anomalies over East Africa during the 1972 drought and 1977–78 wet periods, MSc. thesis, Dep. Meteorol., Univ. of Nairobi, Kenya, 1985.

Morth, H. T., Investigations into the meteorological aspects of the variations in the level of Lake Victoria, *East Afr. Meteorol. Dep. Mem., 4*(2), 1–20, 1967.

Nakamura, K., Equatorial westerlies over East Africa and their climatological significance, *Jpn. Prog. Climatol., 20*, 9–27, 1969.

Nicholson, S. E., The spatial coherence of African rainfall anomalies, Interhemispheric teleconnections, *J. Clim. Appl. Meteorol., 25*, 1365–1381, 1986.

Nicholson, S. E., African drought: Characteristics, causal theories and global teleconnections, in *Understanding Climate Change*, edited by A. Berger, R. E. Dickinson, and J. W. Kidson, pp. 79–100, AGU, Washington, D. C., 1989.

Nicholson, S. E., A review of climate dynamics and climate variability in eastern Africa, Johnson and Odada, pp. 57–78, 1996.

Nicholson, S. E., and D. Entekhabi, Rainfall variability in equatorial and southern Africa: Relationships with sea-surface temperature along the southwestern coast of Africa, *J. Clim. Appl. Meteorol., 26*, 561–578, 1987.

Nicholson, S. E., J. Kim, and J. Hoopingarner, Atlas of African rainfall and its interannual variability, Dep. of Meteorol. Florida State Univ., Tallahassee, 1988.

Ogallo, L. J., Relationships between seasonal rainfall in East Africa and the Southern Oscillation, *J. Clim., 8*, 31–43, 1988.

Ogallo, L. J., Spatial and temporal patterns of the East African rainfall derived from principal component analysis. *Int. J. Clim., 9*, 145–167, 1989.

Ogallo, L. J., J. E. Janowiak, and M. S. Halpert, Teleconnection between seasonal rainfall over East Africa and global sea surface temperature anomalies, *J. Meteorol. Soc. Jpn., 66*, 807–821, 1988.

Ropelewski, C. F., and M. S. Halpert, Global and regional scale precipitation and temperature patterns associated with El Nino/Southern Oscillation, *Mon. Weather Rev., 115*, 1606–1626, 1987.

Shea, D. J., K. E. Trenberth, and R. W. Reynolds, A global monthly sea surface temperature climatology, *J. Clim., 5*, 987–1001, 1992.

Sun, L., H. F. M. Semazzi, F. Giorgi, and L. Ogallo, Application of the NCAR regional climate model to eastern Africa, 1, Simulation of the short rains of 1988, *J. Geophys. Res.*, this issue.

Ward, M. N., Provisionally corrected surface wind data, worldwide ocean-atmosphere surface fields and Sahelian rainfall variability, *J. Clim.*, *5*, 454–475, 1992.

F. Giorgi, National Center for Atmospheric Research, Boulder, CO 80307-3000.

L. Ogallo, Department of Meteorology, Nairobi University, Nairobi, Kenya.

F. H. M. Semazzi, Department of Marine, Earth and Atmospheric Sciences, North Carolina State University, Raleigh, NC 27695-8208. (e-mail: fred-semazzi@ncsu.edu)

L. Sun, Scripps Institution of Oceanography, University of California, San Diego, La Jolla, CA 92037.

(Received February 4, 1998; revised October 5, 1998; accepted October 9, 1998.)